

NANOMETRIC HIGH ASPECT RATIO FILLERS AND CHEMICAL REACTIVITY WITH THE POLYMER MATRIX

Galimberti Maurizio,^a

Cipolletti Valeria,^{ab} Peli Giulia^a, Barbera Vincenzina,^a Bernardi Andrea,^a Locatelli Daniele,^a
Giannini Luca^b

^aPolitecnico di Milano, Department of Chemistry, Materials and Chemical Engineering “G. Natta”, Via Mancinelli 7, 20131 Milano, Italy

^bPirelli Tyre, Via Piero e Alberto Pirelli 25, 20126 Milano

Presented at the 194th Technical Meeting
of the Rubber Division of the American Chemical Society, Inc.
Louisville (KY), October 9 - 11, 2018

ABSTRACT

The research here reported was aimed at improving the compatibility of a high aspect ratio nanometric filler with an elastomer composite. To achieve this goal, the chemical modification of the nanometric filler was performed, preserving the structure of the filler. Sepiolite, a naturally occurring, easily available, low cost clay mineral, with a fibrillar structure, was used as the high aspect ratio nanometric filler. Sepiolite was treated with TEOS in the presence of a basic catalyst obtaining amorphous silica on the surface. Chemical modification was also performed by treating sepiolite with HCl, removing magnesium ions, at an extent depending on the reaction conditions. Chemically modified sepiolites were used in partial replacement of silica in NR based composites and gave the best balance of tensile and dynamic-mechanical properties. This work demonstrates that the chemical modification is a successful approach for enhancing the efficiency, as ingredients of elastomer composites, of nanometric fillers which are not able to occlude polymer chains.

INTRODUCTION

Rubbers achieve the physical mechanical properties required by their applications thanks to reinforcing fillers [1-2].

Carbon black was used already at the beginning of twentieth century [1-2], although its large scale application was delayed by consumer resistance to the black color [3]. Nowadays, besides carbon black, many sp^2 carbon allotropes are efficient reinforcing fillers for rubber materials: carbon nanotubes (CNT), both single [4-5] and multi-walled [6-7], graphene (G) [8-11] or graphitic nanofillers made by few layers of graphene [12-15]. Rationalization of the behaviour of these carbon fillers in rubber composites has been attempted, for carbon nanotubes [16-18] and for graphitic materials [18-21]. Hybrid carbon filler systems have been investigated [22-27].

Silica as well was used in rubber composites at the beginning of last century, but only towards the end its preparation in the precipitated form and the discovery of silane coupling agent [28-29] made silica the best filler for low filler networking and, thus, for low dissipation of energy and fuel consumption [1-2, 30-32]. Inorganic oxides and hydroxides, such as clays and hydrotalcite, have been as well used as efficient fillers in rubber composites, also in hybrid filler systems [18, 26, 33-36].

Reinforcing fillers for rubber composites, grouped above as a function of their chemical nature, are usually classified as nanometric or nanostructured [1-2]. According to the official definition [37], the nanoscale range is approximately from 1 nm to 100 nm and a nanomaterial is a material with any external dimension in the nanoscale or having internal structure or surface structure in the nanoscale. Carbon black and silica are nanostructured fillers: they are made by primary particles with at least one dimension below hundred nanometers, joined together to form aggregates with length of at least 200 nm. Carbon nanotubes, graphene and related materials, clays and

hydrotalcite are nanometric fillers: their nanosized primary particles can be separated and individually dispersed in the polymer matrix.

The importance of nanosize is indicated by the numbers reported in **Table I** below.

TABLE I

Nanosize means larger number of particles per unit volume, larger internal surface area and lower average interparticle distance. In particular, larger surface area means larger filler-polymer interfacial area (i.a.), that means the surface made available by the filler per unit volume of composite, which can be calculated through **Equation 1**, as the product

$$\text{i.a.} = \text{s.a.} * \rho * \phi \quad (1)$$

where s.a. is the surface area, ρ is the filler density and ϕ is the filler volume fraction. Correlation has been revealed between i.a. and both dynamic modulus [38] and vulcanization parameters such as induction time and activation energy [39] for composites based on CB, CNT and the CB/CNT hybrid filler system.

The abovementioned nanometric fillers (CNT, GRM, clays) have high aspect ratio, that means high ratio between their largest and lowest dimensions. Nanometric fillers, thanks to nanosize and high aspect ratio, have very large surface area and can thus establish much larger interaction with the polymer matrix. It is thus clear the interest for nanometric fillers. They can promote the same mechanical properties of rubber composites at much lower content than nanostructured fillers: lightweight materials can be envisaged [25].

However, is the interaction between filler and polymer matrix stable?

In nanostructured fillers, aggregates of carbon black and silica contain voids, which are able to occlude and immobilize part of the polymer matrix: this leads to a stable interaction and is indeed a fundamental contribution to the reinforcement [1-2]. Nanometric fillers do not reveal a structure and immobilization of polymer chains has not been demonstrated. Polymer chains cannot be

accommodated between layers of a graphitic aggregate. Moreover, some of the authors have shown that the intercalation of polymer chains in the interlayer space of a crystalline clay is far from being demonstrated [40-45]. Entangled CNT could trap the chains. However, it has been shown that the tubes are broken during melt blending [46], even by adopting a so called wet melt blending [47]. Hence, it is hard to hypothesize stable polymer occlusion in CNT entanglements. Extensive, labile interaction between filler and polymer chains is expected to lead to high values of modulus at minimum strain and to remarkable modulus decrease as the strain amplitude increases, that means to large Payne effect [48], whatever is the mechanism of such dissipative phenomenon: filler agglomeration–de-agglomeration [49-51] or filler–matrix bonding and debonding [52-60]. Indeed, rubber composites based on clays [44-45, 61]. and CNT [46] have remarkable Payne effect.

Stable interaction between fillers and the polymer matrix can be generated by chemical bonds.

Carbon fillers do not have functional groups suitable to react with rubber chains and not even with other composite ingredients. Reactive carbon fillers would lead to substantial mechanical reinforcement and to dramatic reduction of energy dissipation and hence, for example, of rolling resistance of a tyre compound. Carbon black oxidation was first performed at the end of XIX century. Many efforts have been and are made both in the academic and industrial fields to functionalize carbon fillers [62]. However, functionalized carbon fillers are not yet a large scale industrial reality in the rubber field. In our research group, facile functionalization has been achieved, through different approaches [62-64], in particular by simply reacting an sp^2 carbon allotrope with a pyrrole compound. Solubility parameter of the carbon allotrope was modified in a pretty wide range of values [64]. CB functionalized with 2-(2,5-dimethyl-1*H*-pyrrol-1-yl)-1,3-propanediol (serinol pyrrole) as the pyrrole compound, shown in **Figure 1**, promoted lower Payne effect in compounds based on silica and carbon black.

FIGURE 1

Functionalized high aspect ratio nanofillers, reactive with rubber chains, are not documented in the literature.

Silica is able to establish chemical bonds with diene rubbers thanks to its chemical modification with sulphur based silanes [1-2, 30-32]. The low dissipation of energy of silica based rubber compounds (and hence the low rolling resistance of tyre compounds) is due to the chemical reactivity of silica. Silicates such as clays and inorganic hydroxides such as hydrotalcite do not reveal pronounced chemical reactivity with silanes, due to the relatively low amount and acidity of the OH groups.

The research in our group has been aimed at preparing high aspect ratio nanometric fillers able to establish chemical bonds with the rubber chains. This goal was pursued through the chemical modification of the nanometric fillers, both sp^2 carbon allotropes and inorganic oxides and hydroxides.

In this contribution, for the 94th Meeting of the ACS Rubber Division, the research performed with sepiolite is reported. Sepiolite was selected because is a naturally occurring, easily available, low cost clay mineral, with high mechanical and thermal stability. Its name comes from the greek terms σήπιον (sepion) and λίθος (lithos). They mean, respectively, cuttlebone (the internal porous shell of the cuttlefish) and stone. Indeed, sepiolite resembles to the cuttlebone.

Sepiolite belongs to the sepiolite and palygorskite group [65-67]. Typical of this group is the TOT (tetrahedral-octahedral-tetrahedral) layer-fibrous structure. The sepiolite structure is shown in **Figure 2** below.

FIGURE 2

In the crystals, two-dimensional layers of tetrahedral SiO₄ units (with unshared oxygen atoms facing each other) are joined by magnesium atoms, octahedrally coordinated. The tetrahedral sheet is continuous whereas the octahedral sheet is discontinuous. In such a structure, the TOT units develop indefinitely along the c-axis of the crystal and TOT fragments extend along the a-axis. In the b-axis, the structural units are separated by channels perpendicular to the plane of representation in **Figure 2**, filled with water molecules under ambient conditions. It can thus be said that sepiolite has a *chessboard* structure. The connections in the direction perpendicular to the layers are due, in part, to covalent bonds. Hence, sepiolite and the minerals of this group cannot swell or exfoliate. Crystals of sepiolite are long, very thin, lath-like. Sepiolite laths or fibers are combined to form dense, spongy bundles with 0.1–1 μm diameter. Fibers are typically 40–150 nm wide and 1–10 μm long.

Sepiolite is thus a nanometric filler with high aspect ratio and it could have a relevant effect on the mechanical properties of rubber composites. However, to separate bundles into individual fibers and to promote chemical bonds with polymer chains are indeed challenging tasks. In the scientific literature, composites with sepiolite have been prepared based on polar matrices such as polyamides [68]. The improvement of sepiolite dispersion has been attempted via treatment with ionic liquids [69] and surface modification with methoxysilanes [70].

In this work, two approaches have been adopted to promote the chemical reactivity of sepiolite with unsaturated elastomer chains: (i) formation of nanosilica from tetraethyl orthosilicate on the sepiolite surface (ii) controlled acid treatment of sepiolite, with HCl, aimed at maintaining the morphology and modifying the surface chemistry. The rationale behind these approaches is the following: to promote the formation of Si(OR) and Si(OH) groups on the sepiolite surface, favouring the reaction, for example, with a silane such as the sulphur containing silane bis(3-triethoxysilylpropyl) tetrasulfide (TESPT), typical coupling agent of silica with an unsaturated elastomer. The adopted experimental procedures are presented. Characterization of pristine and modified sepiolite was performed as follows: determining the amount of magnesium in the fiber

through X-ray fluorescence (XRF spectroscopy) and in solution via complexometry, by using thermogravimetric analysis (TGA), Fourier Transformed Infrared spectroscopy in the attenuated total reflection mode (ATR-IR), X-Ray spectroscopy, Field emission scanning electron microscopy (FESEM). Composites based on poly(1,4-*cis*-isoprene) from *Hevea Brasiliensis* were prepared with silica as the main filler, replacing a minor amount of silica with sepiolite, either pristine or modified. Dynamic mechanical properties were investigated through strain sweep tests in the shear mode and tensile properties with quasi static measurements.

EXPERIMENTAL SECTION

Materials

Sepiolite Pangel S9 (SepS9) was from Tolsa and was extracted from the landfill of Vallecas (Spain).

Tetraethyl orthosilicate (98%) and aqueous HCl, 37% by mass, were from Aldrich.

Triethoxy(*n*-octyl) silane ($\geq 97.5\%$) and cyclohexane (99.5%) were from Aldrich.

Poly(1,4-*cis*-isoprene) from *Hevea Brasiliensis* (natural rubber, NR) was SMR GP, with 65 Mooney Units as Mooney viscosity (ML(1+4)100°C), from Lee Rubber.

For the preparation of the elastomeric composites, ingredients were: bis(3-triethoxysilylpropyl)tetrasulfide (TESPT) (Evonik), ZnO (Zincol Ossidi), Stearic acid (Sogis), N-(1,3-dimethylbutyl)-*N*-phenyl-*p*-phenylenediamine (6-PPD) (Crompton), Sulphur (Solfotecnica), *N*-ter-butyl-2-benzothiazyl sulfenamide (TBBS) (Flexyis)

Chemical modification of sepiolite

Treatment of sepiolite with TEOS

In a two-necked round bottomed flask, TEOS (3.22 g) was dissolved in ethanol (15 ml). The solution was heated in an oil bath at 40 °C. Water (0.7 ml) was then dropped from the side neck and the solution was left under stirring for one hour. This solution was then added to a suspension

of sepiolite (5 g) in ethanol (50 ml), previously prepared and stirred or sonicated for 30 min. The bath temperature was raised to 60 °C and ammonia (2 ml) was added dropwise. Vigorous stirring was allowed for 5 hours. Finally, the solid was filtered on a Buchner filter and washed with ethanol, drying the solid in a stove at 70°C.

Treatment of sepiolite with HCl solution

Sample 1. In a 250 ml round bottomed glass flask, 5g of sepiolite were suspended in 50 ml of 1 M HCl aqueous solution. The resulting suspension was heated in an oil bath at 60 °C for 10 minutes under stirring. The suspension was then filtered on a Buchner and the solid was washed with abundant deionized water (about 1.5-2 l) until the washing water was free of chloride ions (AgNO_3 test). The solid was recovered and dried in a stove at 70°C.

Sample 2. The same procedure was followed, except that heating of sepiolite suspension in HCl aq suspension was for 70 minutes.

Reaction of acid treated sepiolite with triethoxy(n-octyl)silane

In a round bottomed flask, 100 ml of cyclohexane and 150 mg of triethoxy(n-octyl)silane were put in sequence. 1.5 g of acid treated sepiolite were then added. The suspension was sonicated at nominal room temperature for 10 minutes. The solvent was then removed first at rotavapor and then with a vacuum pump, for two hours at room temperature. The solid was then heated in a stove for 10 minutes at 150°C. Unreacted silane was extracted from sepiolite/silane adduct with the following procedure. The solid, after the thermal treatment in the stove, was suspended in 30 ml of cyclohexane at room temperature for 16h, filtered and then washed three times with fresh cyclohexane. The amount of silane in the adduct with the silicate was estimated through TGA analysis, from the increase of mass loss of the silanized sample with respect to the pristine silicate, in the range from 300°C and 600°C.

Determination of magnesium present in the fibers by X-ray fluorescence

Spectroscopy was performed by using the Bruker AXS S4 Pioneer XRF spectrophotometer, at room temperature. The powder to be analyzed was placed in a sample holder having a window exposed to incident radiation with a diameter of 34 mm, covered with a 4 micron poly(propene) film. The measurement was carried out in helium at reduced pressure, using the standardless acquisition program "Fast-He34.mm" preset in the instrument, and processing data with the S4tools software using the formula $\text{Si}_6\text{H}_{14}\text{O}\text{R}_{23}$ as a calculation matrix. For greater accuracy, the determination of magnesium was carried out only on the residue after the oxidative treatment in TGA.

Dosage of Mg in the acid reaction medium by complexometry

The magnesium extracted in the reaction medium was measured by using a complexometric method with EDTA [71]. 500 μl of the filtration solution were diluted with 100 ml of distilled water and treated with 4 ml of a solution obtained by dissolving 5.4 g of NH_4Cl in 60 ml of distilled water and 35 ml of aqueous NH_3 at 29% by mass. Two drops of eriochrome black T in 1 % methanol solution were then added to the solution, which was then heated to 40-50 °C and subsequently titrated with disodium EDTA 0.01 M to the turning of the solution colour. The % of extracted Mg was then calculated on the basis of the % of Mg in pristine sepiolite, determined via XRF.

Thermogravimetric analysis (TGA)

TGA was performed with a Mettler Toledo TGA/DSC1 Star-e System, in a temperature range from 150°C to 800 °C. The measurements were carried out by using the following temperature program: (i) from 30°C to 850°C, 10°C/min, in N_2 flow 60 ml min^{-1} (ii) at 850°C isotherm for 10 min, in air, flow 60 ml min^{-1}

Attenuated total reflectance infrared spectroscopy (ATR-IR)

The analyses were carried out with a Perkin Elmer Spectrum 100 (1 cm^{-1} resolution, range of 650-4000 cm^{-1} , 16 scans).

Field emission scanning electron microscopy (FESEM)

It was performed by using a FESEM Ultra Plus Zeiss microscope, Gemini column, in Inlens mode, with excitation of the electron beam from 3.0 to 5.0 KV and working distance from 2.7 to 4.3 mm. Samples to be analyzed were attached to a metal target with adhesive tape and sputtered with gold, to improve electron conductivity. Samples were prepared as follows. 0.005 g of fibers were dispersed in 50 ml of a solution made by water and ethanol, in a mass ratio 8:2, in the presence of 200 ppm of the surfactant Nonidet P40. Treatment with ultrasound in immersion was carried out for 15 minutes. Fibers were separated by centrifugation at 1000 g/m for 20 minutes and dried in stove at 100°C for 3 hours.

X-ray diffraction (XRPD)

The XRD diffraction patterns were taken with a Bruker D8 Avance diffractometer (Cu K-alpha radiation) with 2θ value up to 260 with $\Delta 2\theta = 0.02$ and 4s interval between each acquisition.

Preparation and characterization of elastomer composites

Preparation of elastomer composites

All the quantities of the ingredients are expressed in phr = parts per hundred rubber.

All the ingredients for the non-productive mixing were mixed in an internal mixer for about 5 minutes. As soon as the temperature reached $145\text{ }^{\circ}\text{C} \pm 5\text{ }^{\circ}\text{C}$, the composite was discharged.

Sulphur and TBBS were added on a two roll mill, maintaining the temperature below 60°C.

Dynamic-mechanical characterization

Dynamic-mechanical measurements in the torsion mode were carried out with a Monsanto R.P.A. 2000 rheometer. To cancel the thermo-mechanical history, a first strain sweep (0.1–25% strain amplitude) was performed at 50°C on un-cross-linked samples. To achieve fully equilibrated conditions, the samples were then kept in the instrument at the minimum strain amplitude (0.1%) for 10 min. A strain sweep (0.1–25% strain amplitude) was then performed with a frequency of 1 Hz. Curing was carried out at 150°C with a frequency of 1.67 Hz and an angle of 6.98%. Curing time was 30 min. On cross-linked samples, a first strain sweep (0.1–25% strain amplitude) was performed at 50°C, then the sample was kept in the instrument at the minimum strain amplitude (0.1%) for 10 min, to achieve fully equilibrated conditions. Finally, a strain sweep (0.1–25% strain amplitude) was performed with a frequency of 1 Hz.

Tensile properties

Tensile measurements were determined on samples of the elastomeric compositions vulcanized at 150°C for 30 minutes. Stresses at 10, 50, 100 and 300% of elongation (σ_{10} , σ_{50} , σ_{100} and σ_{300} respectively), stress at break (σ_b) and elongation at break (ϵ_B) were measured according to Standard ISO 37:2005.

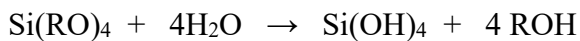
RESULTS AND DISCUSSION SECTION

Treatment of sepiolite with TEOS

Preparation and characterization of sepiolite modified with TEOS

The treatment with TEOS was aimed at forming amorphous nanosilica on the surface of sepiolite. The preparation of nanosilica from TEOS is well documented in the literature, with the help of either basic or acid catalysts [72]. In the present work, it was applied the Stober method, a sol gel process [73] which allows to obtain silica particles of controlled and uniform size [74-77]. Tetraethyl orthosilicate, the silica precursor, is hydrolyzed in alcohol with ammonia as the

catalyst: a mixture of ethoxysilanol and ethanol are produced. Silanols can then condense with either other silanols or TEOS, forming silica. The hydrolysis reaction leading to Si(OH)_4 and the successive condensation reaction to SiO_2 are reported as follows.



In the literature [78], it was reported a kaolinite covered with silane-grafted silica, used as filler for styrene-butadiene rubber. However, documents on fibrillar silicates modified with sol-gel silica are not available.

Treatment of sepiolite with TEOS was performed as described in detail in the Experimental Section and summarized in the Scheme in **Figure 3**.

FIGURE 3

In brief, TEOS was dissolved in ethanol, water was added and stirring was performed at moderate temperature (40°C) for 1 hour. 3.22 g of TEOS are equivalent to 0.87 g of amorphous silica. Such a mixture was added to a suspension of sepiolite in ethanol, previously sonicated for 30 minutes. Ammonia was then added and the resulting suspension was stirred at 60°C for 5 hours. The solid product was filtered on a Buchner and washed with ethanol. The resulting modified sepiolite was then characterized by means of TGA, IR, RX, FESEM analyses.

Results of TGA analysis are shown in **Figure 4**. Values of mass losses (indicated also in **Figure 4**) are in **Table 2**.

FIGURE 4

TABLE II

The mass losses observed in TGA graph of pristine sepiolite were interpreted with the help of what reported in the scientific literature [79, 80]. At $T < 150^{\circ}\text{C}$: absorbed water. In the range $150 < T < 400$: coordinated water. In the range $400 < T < 700$: water trapped in the sepiolite channels. In the range $700 < T < 850$: de-hydroxylation of Mg-OH groups. The sepiolite/TEOS reveals lower mass loss in the range $150 < T < 400$ and larger mass loss in the range $400 < T < 700$. These differences in mass loss allow to hypothesize the presence of an organic compound in the sepiolite/TEOS composite. Indeed, the mass loss in the range at higher temperatures is typical of a silane grafted on silica.

ATR-IR was performed on pristine sepiolite and on sepiolite/TEOS. The spectra, in the range from about 2800 to about 3800 cm^{-1} are shown in **Figure 5**.

FIGURE 5

In Spectra in **Figure 5**, peaks are in particular indicated at following wavelengths: about 3516 cm^{-1} (1), about 2980 and 2903 cm^{-1} (2). In the spectrum of sepiolite/TEOS, it is possible to observe: (i) at about 3516 cm^{-1} , the reduction of the intensity of the peak due to H_2O coordinated to the octahedral layers of sepiolite, (ii) at about 2980 and 2903 cm^{-1} peaks due to the stretching of $-\text{CH}_2$ coming from TEOS. Moreover, in the spectral region of the Si-O-Si stretching (not shown in the figure), shift of peaks has been observed from about 1006 and 973 to about 1011 and 971, passing from pristine sepiolite to sepiolite/TEOS. These findings suggest that sepiolite was modified by TEOS.

X-ray were taken on pristine sepiolite and on sepiolite/TEOS. Patterns are shown in **Figure 6**.

FIGURE 6

Typical reflections are in the pattern of pristine sepiolite [81]. In the pattern of sepiolite/TEOS, it is possible to notice a halo, indicated by the arrow, which could be attributed to amorphous silica. Pictures taken with FESEM on pristine sepiolite and sepiolite/TEOS are in **Figure 7**, (a) and (b) respectively.

FIGURE 7

Micrograph in **Figure 7(a)** reveals the typical fibrillar shape of pristine sepiolite. **Figure 7(b)** shows silica nanoparticles on sepiolite fibrils.

Composites based on NR, silica and sepiolite modified with TEOS

Data on the use of sepiolite modified with TEOS as filler for elastomer composites are available in a patent by some of the authors [82].

Composites were prepared based on NR as the rubber and silica as the main filler. Partial replacement (10 phr on a total amount of 45 phr) of silica was performed with either pristine sepiolite or with sepiolite modified with TEOS. Silica was replaced with the same mass amount of sepiolite, taking also into consideration that the densities of silica and sepiolite are pretty close to each other (silica density: 2.00 g/cm³, sepiolite density: 2.30 g/cm³). Formulations are shown in **Table 3**.

TABLE III

Preparation of composites was performed as described in the Experimental Section.

Dynamic-mechanical properties were determined by performing strain sweep tests in the shear

mode. Values of G' , $\Delta G'/G'$, Tan Delta max are in **Table IV**.

TABLE IV

The replacement of silica with pristine sepiolite does not lead to a really appreciable variation of the dynamic-mechanical properties. A slight worsening of the hysteretic properties can be observed. Lower values of $G'_{\gamma_{min}}$, $\Delta G'/G'$ and Tan delta max were obtained by using sepiolite/TEOS.

Results obtained from tensile and measurements are reported in **Table V**: stresses at 50%, 100% and 300% of elongation (σ_{50} , σ_{100} and σ_{300} respectively), stress at break (σ_b), elongation at break (ϵ_B).

TABLE V

The partial replacement of silica with sepiolite leads to larger values of stress, at all elongations. In particular, large values at low strains are obtained with pristine sepiolite.

A comparative analysis of data in **Table IV** and in **Table V** reveals that the best combination of dynamic-mechanical and static properties is obtained with the sepiolite treated with TEOS.

Treatment of sepiolite with acid

Treatment and characterization

The treatment of sepiolite with acid was aimed at partial removal of magnesium, preserving the needle-shaped morphology of the fibers and creating silica only at surface level. Upon achieving this goal, sepiolite fibers with larger reactivity, for example with sulphur containing silanes, would be available.

Acid treatment processes of silicate fibers, in particular of sepiolite, are documented in the

literature [80, 83-85]. Conditions of acid treatment affect the extent of magnesium removal and the final structure of the silicate: more drastic conditions lead to larger magnesium removal and to conversion of fibers into amorphous silica. It is reported [85] that the extraction of peripheral magnesium (up to about 33%) does not remarkably affect the crystalline structure, which collapses when also magnesium in the internal part of the crystal is extracted.

Before performing the research here reported, documents were not available on the use in elastomeric composites of acid treated sepiolite with preserved high aspect ratio. Indeed, sepiolite fibers were subjected to treatments with 6M nitric acid and samples of amorphous silica with different surface area were obtained and used in SBR based composites [86]. An amorphous silica with a high surface area and less than 1% residual Mg, was used in elastomer composites [87].

People of the research group recently published on the use of acid treated sepiolite in elastomer composite, focusing the attention on the size-controlled self-assembly of the anisotropic fibers [88]. Data are available in the patent literature [89].

The experimental conditions adopted in the present work for the treatment of sepiolite are reported in the experimental section and summarized in **Figure 8** below.

FIGURE 8

Two samples are here described, obtained by heating the sepiolite suspension in HCl solution at 60°C for 10 and 70 minutes.

Samples of sepiolite treated with HCl were characterized by determining the amount of Mg content and by means of TGA, IR, RX, FESEM analyses.

The determination of magnesium content in sepiolite was performed by XRF spectroscopy, as described in the experimental part. Magnesium in pristine sepiolite was about 6.3 mmol/g of sepiolite. The amount of extracted magnesium, in the extraction solution, was determined with a complexometric method with EDTA, described in detail in the Experimental Section. The % by

mass of extracted magnesium was calculated with respect to the total mass of the magnesium present in pristine sepiolite. Results are in **Table VI**.

TABLE VI

Under the adopted experimental conditions (3M HCl aq solution, 60°C), the amount of extracted magnesium dramatically depended on the extraction time. More than 30% was extracted after 10 minutes and more than 80% after 70 minutes.

Results of TGA analysis are shown in **Figure 9**: Fig. 9a for Sample 1, treated with HCl for 10 minutes and Fig. 9b, treated with HCl for 70 minutes.

FIGURE 9

Quantitative data on mass losses and residues are in **Table VII**.

TABLE VII

Treatment with acid leads to lower mass losses in TGA analysis. Slight difference is observed for Sample 1, treated for 10 minutes, with an extracted magnesium of about 30%.

In the case of Sample 2 (sepiolite treated with HCl for 70 min), with % of extracted magnesium larger than 80%, are observed only the mass losses due to absorbed water and to de-hydroxylation of Mg-OH groups and, probably, also of silanols.

ATR-IR was performed, in the Attenuated Total Reflectance mode, on pristine sepiolite and on sepiolite treated with acid, both Sample 1 (10 min at 60°C) and Sample 2 (70 min at 60°C). The spectra, in the range from about 3000 to about 3800 cm^{-1} are shown in **Figure 10**.

FIGURE 10

The treatment with acid leads to a reduction of the intensity of bands at 3688 cm^{-1} and 3566 cm^{-1} , due to hydroxyl groups bound to Mg (3688 cm^{-1}) and to water molecules bound to the octahedral Mg layers (3566 cm^{-1}), in the spectrum of Sample 1. These bands cannot be detected in the spectrum of Sample 2.

X-rays were taken in the 2θ region between 2° and 50° on pristine sepiolite, on Sample 1 and Sample 2. Patterns are shown in **Figure 11**.

FIGURE 11

Attention can be focused on the 110 reflection of pristine sepiolite. Such reflection is still present in the pattern of Sample 1, whereas cannot be detected in the pattern of Sample 2. These findings confirm that treatment of sepiolite with HCl at 60°C for 10 minutes allows to maintain the crystalline structure, whereas the treatment for 70 brings to an amorphous silicate.

FESEM was performed on pristine sepiolite and on samples treated with acid. Pictures are in **Figure 12**.

FIGURE 12

The fibrillar structure of sepiolite is preserved after the treatment with acid for 10 min, whereas shorter fibrils and globular silicate particles can be observed in the micrograph of Sample 2, treated for 70 min.

*Reaction of acid treated sepiolite with triethoxy(*n*-octyl)silane*

The treatment of sepiolite with acid was also aimed at improving the reactivity of sepiolite with

the sulphur based silane TESPT. In order to check if the acid treatment was successful for increasing the reactivity of sepiolite with a silane, the reaction of acid treated sepiolite (Sample 1, treated at 60°C for 10 min) with triethoxy(n-octyl)silane was studied. The adopted procedure is in the Experimental Section. In brief, sepiolite was impregnated with the silane (10% by mass) and was then kept at 150°C for 10 minutes. The resulting product was washed with cyclohexane. The same procedure was adopted, for comparison, with pristine sepiolite and silica. The amount of silane in the adduct with the silicate was estimated through TGA. Data on the % of silane left on the silicate after thermal treatment are in **Table VIII**.

TABLE VIII

Acid treatment promotes larger reactivity of sepiolite with silane. The amount of silane found in the final product is even close to the amount found on silica.

The sample treated first with acid (Sample 1) and then with triethoxy(n-octyl)silane was analysed with ATR-IR. Patterns of pristine and modified sepiolite are in **Figure 13**.

FIGURE 13

The IR spectrum of acid treated sepiolite (Sample 1) silanized with triethoxy(n-octyl)silane reveals the bands typical stretching of CH and CH₂ (2964 cm⁻¹; 2856 cm⁻¹)

Composites based on NR, silica and sepiolite treated with acid

Composites were prepared based on NR as the rubber and silica as the main filler. Partial replacement (10 phr on a total amount of 45 phr) of silica was performed with either pristine sepiolite or with sepiolite treated with acid. Sample 1 was used, with 33% of extracted magnesium and preserved fibrillar shape. Formulations adopted for the composites are in **Table IX**. As

already commented for composites with sepiolite/TEOS, silica was replaced with the same mass amount of sepiolite.

Preparation of the composites was performed analogously to what done for composites of Table III, as described in detail in the Experimental Section.

TABLE IX

Dynamic-mechanical properties were determined by performing strain sweep tests in the shear mode. Values of G' , $\Delta G'/G'$, Tan Delta max are in **Table X**.

TABLE X

The replacement of silica with pristine sepiolite does not lead to a really appreciable variation of the dynamic-mechanical properties. Only a slight worsening of the hysteretic properties can be observed. In the case of the composite containing the acid treated sepiolite, lower values of $G'_{\gamma_{min}}$, $\Delta G'/G'$ and Tan delta max were obtained.

Results from tensile and measurements are reported in **Table XI**: stresses at 10%, 50%, 100% and 300% of elongation (σ_{50} , σ_{100} and σ_{300} respectively), stress at break (σ_b) and elongation at break (ϵ_B).

TABLE XI

The replacement of a minor amount of silica with pristine sepiolite leads to a composite with larger mechanical reinforcement, particularly at low strains. The presence in the composite of the acid treated sepiolite leads as well to larger values of stresses at low strain and brings about better ultimate properties.

A comparative analysis of data in **Table IX** and in **Table X** reveals that the best combination of dynamic-mechanical and static properties is obtained with the acid treated sepiolite, with preserved fibrillar structure.

CONCLUSIONS

The chemical modification of sepiolite was achieved, preserving the fibrillar structure of the silicate. Sepiolite was treated with tetraethyl orthosilicate, in the presence of a basic catalyst, forming amorphous silica on the sepiolite surface. Sepiolite was also treated with HCl, obtaining the removal of magnesium: samples with 33% and 70% of removed magnesium were studied, the former with preserved fibrillar shape. Acid treated sepiolite revealed larger reactivity with a silane, such as triethoxy(n-octyl)silane.

Sepiolite treated either with TEOS or with acid was used in NR based composites, in partial replacement of silica. The comparison with pristine sepiolite revealed that the modified fibrils gave the best balance of static and dynamic-mechanical properties. These results can be reasonably interpreted with the chemical reactivity of modified sepiolite, in particular with the Sulphur based silane TESPT.

This work reveals that it is indeed possible to promote the compatibility of a high aspect ratio nanometric filler in an elastomeric composite, also in the case of fillers which are not able to occlude polymer chains. This can be achieved with the chemical modification of the nanometric filler. In this work, silanol groups were introduced on sepiolite, promoting its reactivity with the composite ingredients and with the polymer matrix.

REFERENCES

- [1] Medalia A.I., Kraus G., in *The Science and Technology of Rubber* Second Ed.; Mark, J.E.; Erman, B.; Eirich, F.R. Eds. Elsevier Academic Press **1994**, Chapter 8, 387-418

- [2] Donnet J.B., Custodero E., in *The Science and Technology of Rubber* Third Ed.; Mark, J.E.; Erman, B.; Eirich, F.R. Eds. Elsevier Academic Press **2005**, Chapter 8, 367-400
- [3] Schidrowitz, P.; Dawson, T.R.; *History of the Rubber Industry*, Heffer, Cambridge, **1952**, 71-72.
- [4] Iijima S., Ichihashi T., *Nature*, **1993**; 363-603.
- [5] Bethune D.S., Kiang C.H., de Vries M.S., Gorman G., Savoy R., Vazquez J. et al., *Nature*, **1993**, 363-605
- [6] Iijima S., *Nature*, **1991**, 354-356.
- [7] Monthieux M., Kuznetsov V.L., *Carbon*, **2006**; 44(9), 1621-1623.
- [8] Novoselov K. S., Geim A. K., Morozov S. V., Jiang D., Zhang Y., Dubonos S. V., Grigorieva I. V., Firsov A. A., *Science*, **2004**, 306, 666–669.
- [9] Geim A. K. and Novoselov K. S., *Nat. Mater.*, **2007**, 6(3), 183–191.
- [10] Allen M. J., Tung V. C. and Kaner R. B., *Chem. Rev.*, **2010**, 110, 132–145.
- [11] Zhu Y. W. et al., *Adv. Mater.*, **2010**, 22, 3906–3924.
- [12] Geng Y., Wang S. J. and Kim J.-K., *J. Colloid Interface Sci.*, **2009**, 336(2), 592–598.
- [13] Kavan L., Yum J. H. and Gratzel M., *ACS Nano*, **2011**, 5, 165–172.
- [14] Nieto A., Lahiri D. and Agarwal A., *Carbon*, **2012**, 50(11), 4068–4070.
- [15] Paton K. R., Varrla E., Backes C., Smith R. J., Khan U., O'Neill A., Boland C., Lotya M., Istrate O. M., King P., Higgins T., Barwich S., May P., Puczkarski P., Ahmed I., Moebius M., Pettersson H., Long E., Coelho J., O'Brien S. E., McGuire E. K., Mendoza Sanchez B., Duesberg G. S., McEvoy N., Pennycook T. J., *Nat. Mater.*, **2014**, 13, 624–630.
- [16] Bokobza L.. *POLYMER*. **2007**, 48, 4907
- [17] Maiti M., Bhattacharya M., Bhowmick A. K., *RUBBER CHEM. TECHNOL.* **2008**, 81, 384
- [18] Galimberti M., Cipolletti V., Musto S., Cioppa, S. Peli G., Mauro M., Guerra G., Agnelli S., Riccò T., Kumar V., *RUBBER CHEMISTRY AND TECHNOLOGY* **2014**, 87. 417, 3 .

- [19] Bhattacharya M., Maiti M., Bhowmick AK., POLYMER ENGINEERING & SCIENCE. **2009**, 49, 81
- [20] Bhowmick AK., Bhattacharya M., Mitra S., JOURNAL OF ELASTOMERS AND PLASTICS. **2010**, 42, 517
- [21] Al-Solamya F.R., Al-Ghamdib A. A., Mahmou W.E., *POLYMER FOR ADVANCED TECHNOLOGY*, **2012**, 23, 478
- [22] Galimberti M., Kumar V., Coombs M., Cipolletti V., Agnelli S., Pandini S., Conzatti L., *Rubber Chemistry and Technology*, **2014**, 87(2), 197-218
- [23] Agnelli S., Cipolletti V., Musto S., Coombs M., Conzatti L., Pandini S., Riccò T., Galimberti M., *eXPRESS Polymer Letters* **2014**, 8(6), 436-449
- [24] Galimberti M., Cipolletti V., Agnelli S., Pandini S., *Rubber World*, **2017**, 28-37
- [25] Galimberti M., Infortuna G., Guerra S., Barbera V., Agnelli S., Pandini S., *eXPRESS Polymer Letters* **2018**, 12(3) 265–283
- [26] Galimberti M., Agnelli S., Cipolletti V., "Hybrid filler systems in rubber nanocomposites" in the Book "Progress in Rubber Nanocomposites 1st Edition" Hardcover ISBN: 9780081004098, eBook ISBN: 9780081004289, Editors: Sabu Thomas Hanna Maria Imprint: Woodhead Publishing, Published Date: 10th November **2016**, Page Count: 596
- [27] Galimberti M., Infortuna G., Barbera V., Guerra S., Bernardi A., Agnelli S., Pandini S., *Rubber World*, **2018**, 257(5), 24-30
- [28] Voet A., Morawski, J.C., Donnet J.B., *Rubber Chem. Technol.* **1977**, 50, 342
- [29] Rauline R., EP 501227 to Compagnie Generale des Etablissements Michelin **1991**
- [30] Leblanc J. L., Rubber–filler interactions and rheological properties in filled compounds Progress in Polymer Science, Volume 27, Issue 4, May **2002**, Pages 627-687
- [31] Schwaiger B, Blume A, *Rubber World*, **2000** 222(1) 32-38

- [32] Sato, M., Dierkes, W. K., & Blume, A. Silane-polymer reaction: Investigation of the silane-polymer reaction in a model system. *Tire technology international*, 2017(Annual showcase), 66-70, **2017**
- [33] Paul D. R., Robeson L. M., *POLYMER*, **2008**, 49, 3187
- [34] Galimberti M., *RUBBER CLAY NANOCOMPOSITES: SCIENCE, TECHNOLOGY, APPLICATIONS*. John Wiley and Sons, **2011**.
- [35] Galimberti M., Cipolletti V., Kumar V., “Natural Rubber Materials: Volume 2: Composites and Nanocomposites”, eds. S. Thomas, C.H. Chan, L. Pothan, J. Joy, H. Maria, Royal Society of Chemistry, **2013**.
- [36] M. Galimberti, V. Cipolletti, M. Coombs, *HANDBOOK OF CLAY SCIENCE* 4.4. **2013**
- [37] ISO/TS 80004-1:2015(en)
- [38] Agnelli S., Cipolletti V., Musto S., Coombs M., Conzatti L., Pandini S., Riccò T., Galimberti M., *eXPRESS Polymer Letters*, **2014**, 8(6), 436.
- [39] Musto S., Barbera V., Cipolletti V., Citterio A., Galimberti M., *eXPRESS Polymer Letters*, **2017**, 11(6), 435–448.
- [40] M. Galimberti, A. Lostritto, A. Spatola, G. Guerra, *Chemistry of Materials*, **2007**, 19, 2495–249
- [41] Galimberti M., Senatore S., Conzatti L., Costa G., Giuliano G., Guerra G., *Polym. Adv. Technol.* **2009**, 20, 135-142
- [42] Galimberti M., Giudice S., Cipolletti V., Guerra G., *Polymers for Advanced Technologies* **2010**, 21 679–684
- [43] Cipolletti V., Galimberti M., Mauro M., Guerra G., *Applied Clay Science*, **2014**, 87, 179-188
- [44] Galimberti M., Coombs M., Cipolletti V., Spatola A., Guerra G., Lostritto A., Giannini L., Pandini S., Riccò T., *Applied Clay Science* **2014**, 97, 8-16
- [45] Galimberti M., Coombs M., Pandini S., Riccò T., Cipolletti V., Conzatti L., Guerra G., *Applied Clay Science* **2015**, 104, 8–17

- [46] Galimberti M., Coombs M., Riccio P., Riccò T., Passera S., Pandini S., Conzatti L., Ravasio A., Tritto I., *Macromol. Mater. Eng.*, **2012**, 298, 241-251.
- [47] Das A., Stockelhuber K.W., Jurk R., Saphiannikova M., Fritzsche J., Lorenz H., Kuppler M., Heinrich G., *Polymer* **2008**, 49, 5276 - 5283
- [48] Payne A. R., Whittaker R. E.: *Rubber Chemistry and Technology*, **1971**, 44, 440 – 478
- [49] Robertson C.G., Roland C.M.: *Rubber Chemistry and Technology*, **2008**, 81, 506 – 522 (2008).
- [50] Bohm G.A., Tomaszewski W., Cole W., Hogan T.: *Polymer*, **2010**, 51, 2057 – 2068.
- [51] Heinrich G., Kluppel M., *Adv. Polym. Sci.*, 160, 1
- [52] Maier P.G., Goritz D.: *Kautschuk Gummi Kunststoffe*, **1996**, 49, 18 – 21.
- [53] Chazeau L., Brown J.D., Yanyo L.C., Sternstein S.S.: *Polymer Composites*, **2000**, 21, 202 – 222 (2000).
- [54] Sternstein S.S., Zhu A.J.: *Macromolecules*, **2002**, 35, 7262 - 7273 (2002).
- [55] Montes H., Lequeux F., Berriot J.: *Macromolecules*, **2003**, 36, 8107 – 8118 (2003).
- [56] Zhu Z., Thompson T., Wang S. Q., von Meerwall E. D., Halasa A.: *Macromolecules*, **2005**, 38, 8816 – 8824.
- [57] Kalfus J., Jancar J.: *Polymer Composites*, **2007**, 28, 365-371 (2007).
- [58] Jancar J., Douglas J.F., Starr F.W., Kumar S.K., Cassagnau P., Lesser A.J., Sternsteinh,S.S., Buehler M.J.: *Polymer*, **2010**, 51, 3321-3343.
- [59] Funt J.M.: *Rubber chemistry and technology*, **1988**, 61, 842-865.
- [60] Gauthier C., Reynaud E., Vassoille R., Ladouce-Stelandre L.: *Polymer*, **2004**, 45, 2761–2771
- [61] Galimberti M., Senatore S., Lostritto A., Giannini A., Conzatti L., Costa G., Guerra G., *e-Polymers* , **2009**, 057, 1-16
- [62] Galimberti, M., Barbera, V., Guerra, S., & Bernardi, A. *Rubber Chemistry and Technology*, **2017**, 90(2), 285-307.

- [63] Barbera, V., Bernardi, A., Torrisi, G., Porta, A., & Galimberti, M. *Elastomery*, **2017**, 21.
- [64] Barbera, V., Bernardi, A., Palazzolo, A., Rosengart, A., Brambilla, L., & Galimberti, M.. *Pure and Applied Chemistry*, **2018**, 90(2), 253-270.
- [65] Murray, H.H., *Applied Clay Mineralogy: Occurrences, Processing and Application of Kaolins, Bentonites, Palygorskite-Sepiolite, and Common Clays*. Elsevier, Amsterdam. *Articolo sepiolite*, **2007**.
- [66] Miles, J.W., Amargosa sepiolite and saponite: geology, mineralogy, and markets. In: *Developments in Clay Science. Developments in Palygorskite-Sepiolite Research 3*. pp. 583–621, **2006**.
- [67] F. Bergaya, M. Jaber, J.F. Lambert, Natural and synthetic layered clays sepiolite, Chapter 1 in Galimberti, M.,. *Rubber-Clay Nanocomposites*. Wiley. **2011**
- [68] Fernandez-Barranco, C., Koziół, A.E., Szypiec, K., Rawski, M., Drewniak, M., YebraRodriguez, A., *Appl. Clay Sci.* **2016**, 127–128, 129–133
- [69] DeLima, J., Camilo, F.F., Faez,R., Cruz, S.A., *Appl. Clay Sci.* **2017**, 143, 234–240.
- [70] García, N., Guzman, J., Benito, E., Esteban-Cubillo, A., Aguilar, E., Santaren, J., Tiemblo, P.,. *Langmuir* **2011**, 27, 3952–3959.
- [71] Hernández, L. G., Rueda, L. I., Diaz, A. R., & Antón, C. C. *Die Angewandte Makromolekulare Chemie: Applied Macromolecular Chemistry and Physics*, **1982**, 103(1), 51-60.
- [72] Iler R.K., *The Chemistry of Silica*, Wiley, New York, **1979**
- [73] Stöber, W., Fink, A.; Bohn, E. " *Journal of Colloid and Interface Science*. **1968**, 26 (1): 62–69,
- [74] Bogush, G.H.; Tracy, M.A.; Zukoski, C.F. *Journal of Non-Crystalline Solids*. **1988**, 104 (1): 95–106,
- [75] Brinkler C., Scherer G., *Sol-Gel Science: The Physics and Chemistry of Sol-Gel Processing*. Academic Press, Boston, MA, **1990**

- [76] Van Blaaderen, A., Van Geest, J., & Vrij, A. *Journal of colloid and interface science*, **1992**, 154(2), 481-501.
- [77] Corriu, R., Trong Anh, N., *Molecular Chemistry of Sol Gel Derived Nanomaterials*, Wiley, **2009**
- [78] Zhang, Q., Liu, Q., Zhang, Y., Cheng, H., & Lu, Y. *Applied Clay Science*, **2012**, 65, 134-138.
- [79] Nagata, H., Shimoda, S., & Sudo, T. On dehydration of bound water of sepiolite. In *Clays & Clay Minerals*, **1974**.
- [80] Valentin, J.L., M.A. López-Manchado, A. Rodríguez, P. Posadas, L. Ibarra et al. *Applied Clay Science*, **2007**, 36(4), 245-255
- [81] A Preisinger X-ray study of the structure of sepiolite *Clays and Clay Minerals*, **1959**, 61-67
- [82] Giannini, L., Galimberti, M., Cipolletti, V., Peli, G., Vulcanisable elastomeric materials for components of tyres comprising modified silicate fibres, and tyres thereof. WO 2016/174628 A1
- [83] Myriam, M., Suarez, M., & Martin Pozas, J. M., *Clays and clay minerals*, **1998**, 46(3), 225-231.
- [84] Balci S., *Clay Minerals*, **1999**, 34(4) 647-655
- [85] Esteban-Cubillo, A., Pina-Zapardiel, R., Moya, J. S., Barba, M. F., & Pecharromán, C. *Journal of the European Ceramic Society*, **2008**, 28(9), 1763-1768.
- [86] Rueda, L. I., Hernández, L. G., & Anton, C. C., *Polymer composites*, **1988**, 9(3), 204-208.
- [87] Hernández L. G., Rueda L. I., Diaz A. R., & Antón, C. C., *Die Angewandte Makromolekulare Chemie: Applied Macromolecular Chemistry and Physics*, **1982**, 103(1), 51-60.
- [88] Di Credico B., Cobani E., Manuela Callone E., Conzatti L., Cristofori D., D'Arienzo M., Dirè S., Giannini L., Hanel T., Scotti R., Stagnaro P., Tadiello L., Morazzoni F., *Applied Clay Science*, **2018**, 152, 51-64

- [89] Giannini, L., Tadiello, L., Hanel, T., Galimberti, M., Cipolletti, V., Peli, G., Morazzoni, F., Scotti, R., Di Credico, B., Vulcanisable elastomeric materials for components of tyres comprising modified silicate fibres, and tyres thereof. WO 2016/174629 A1

FIGURE 1

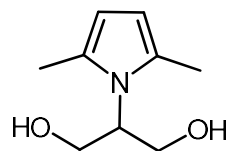


FIGURE 2

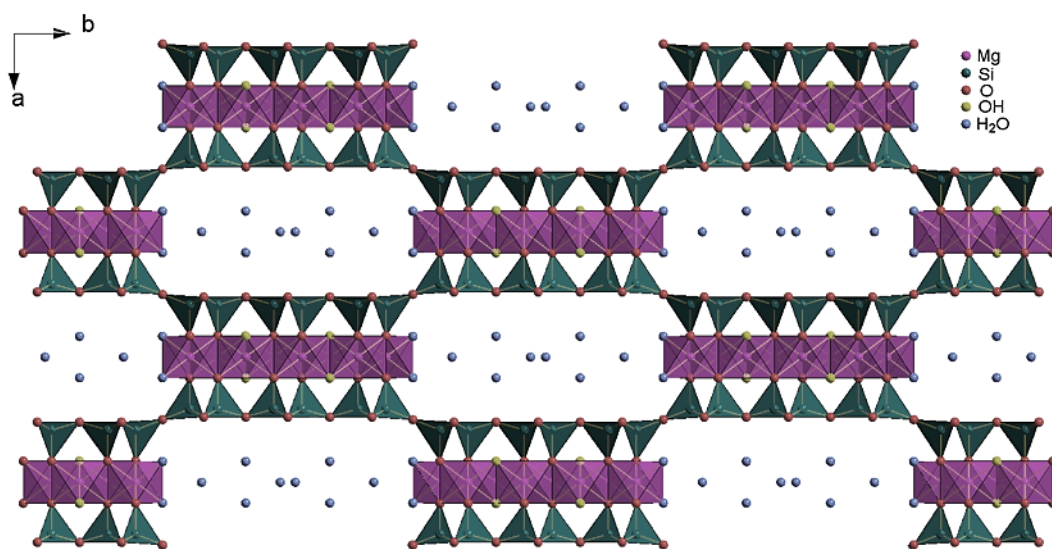


FIGURE 3

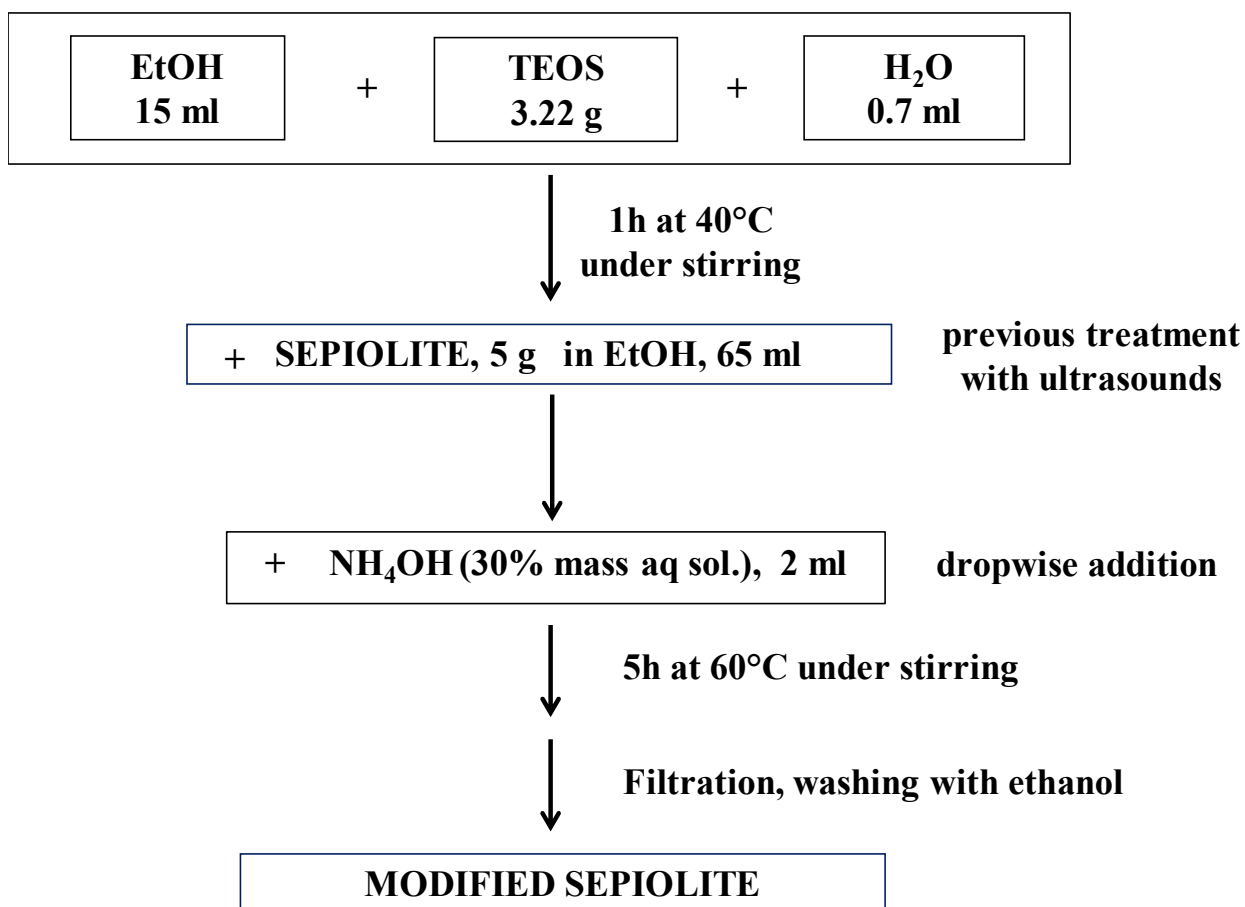


FIGURE 4

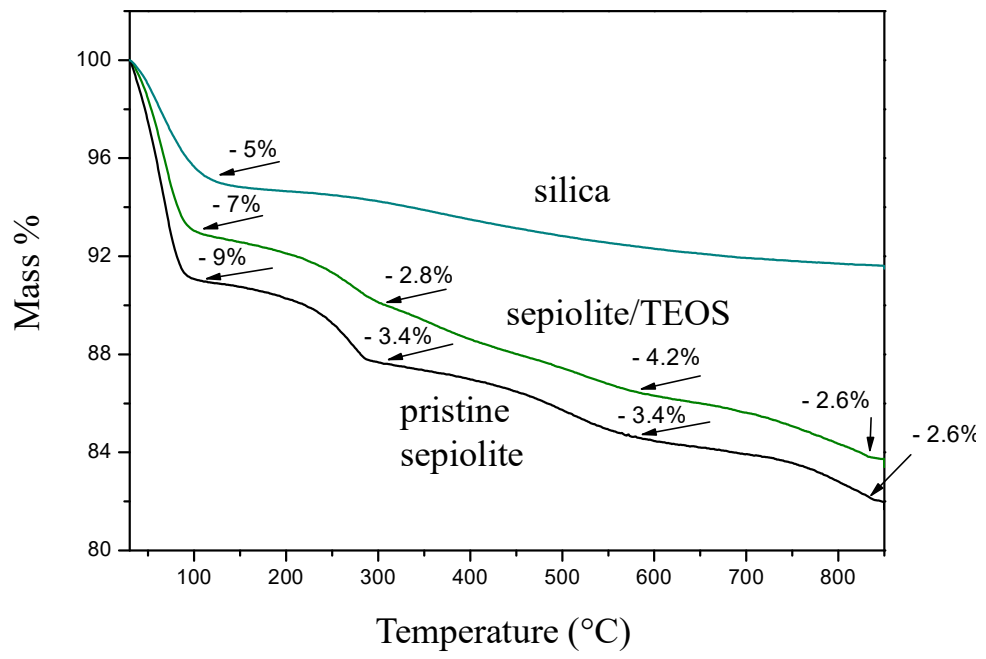


FIGURE 5

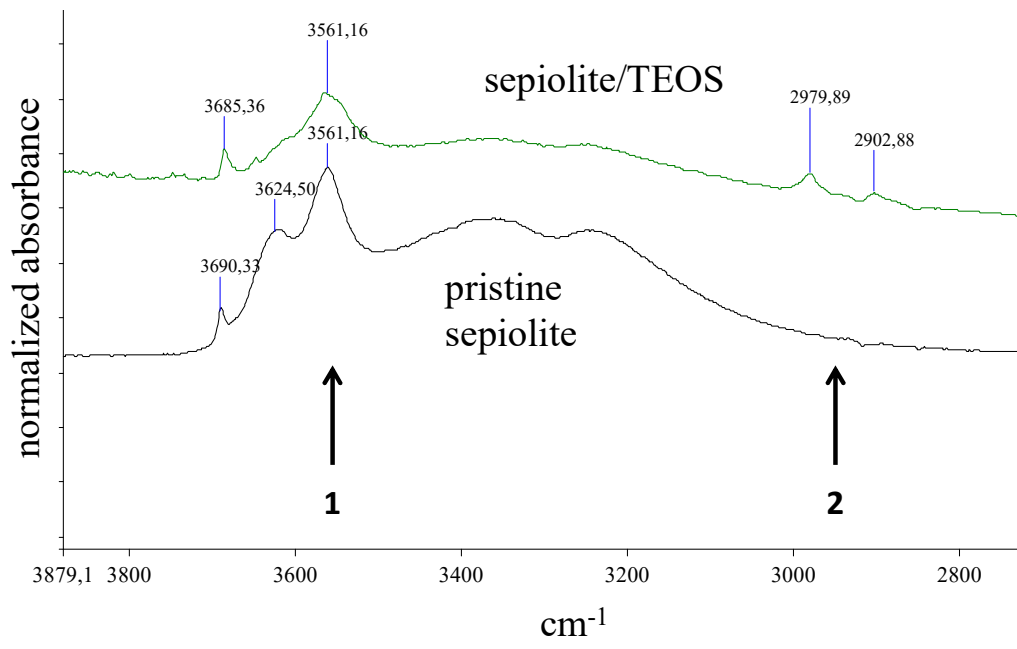


FIGURE 6

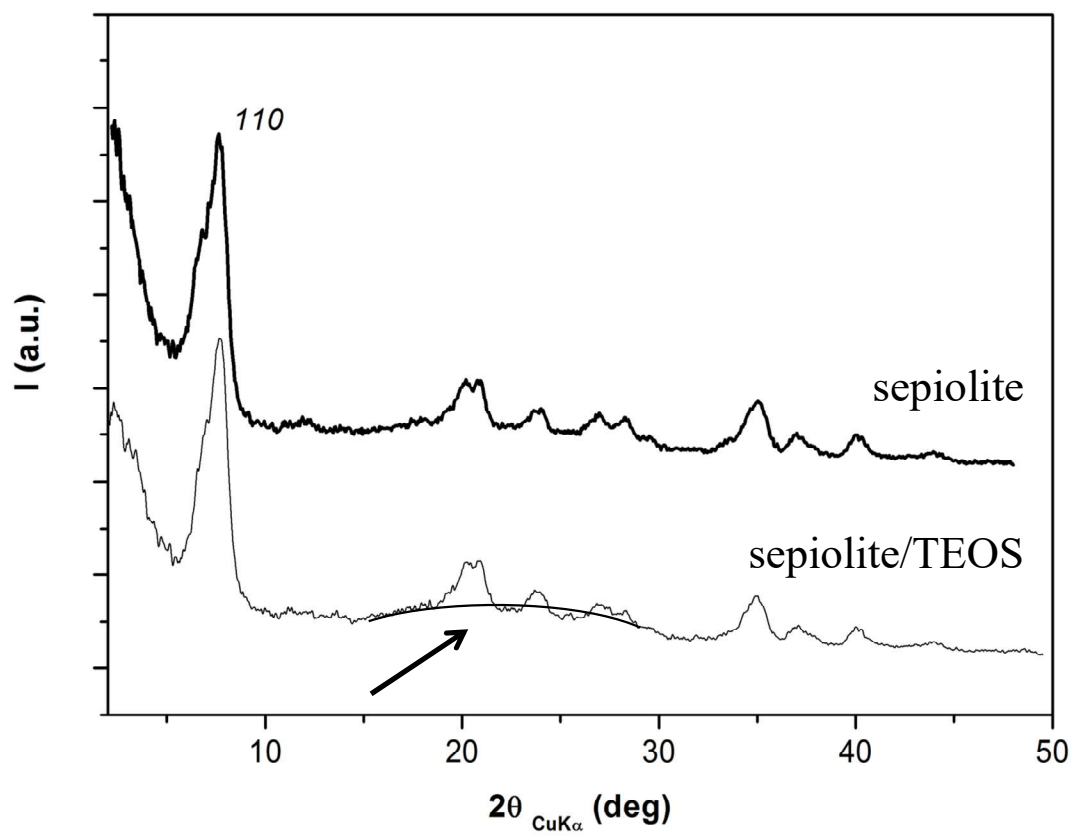


FIGURE 7

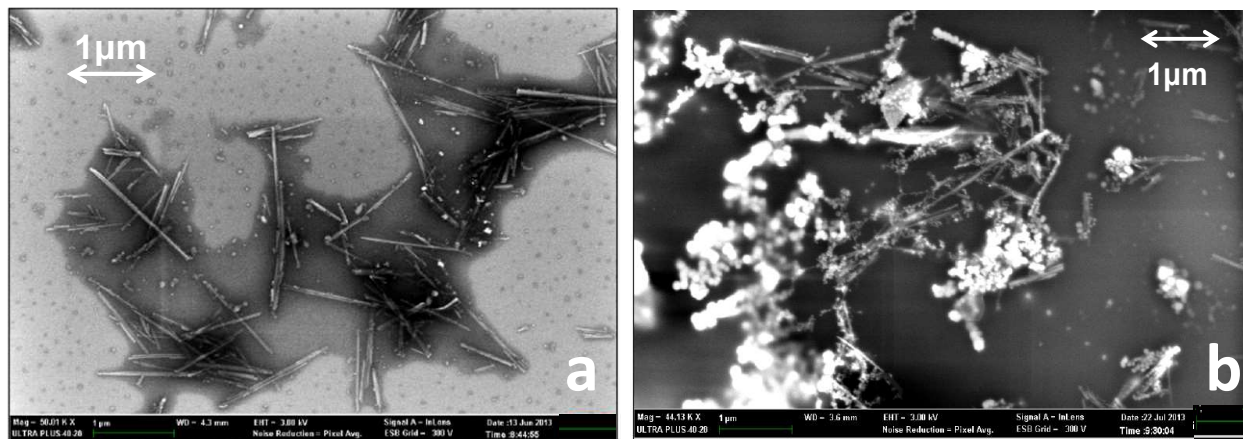


FIGURE 8

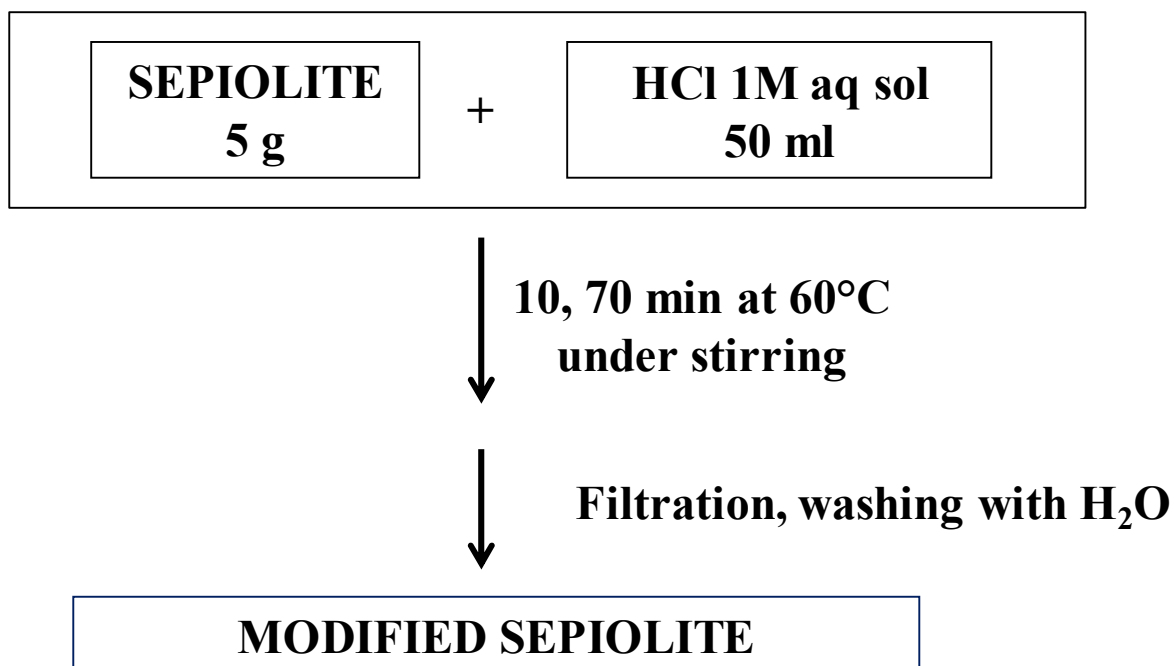


FIGURE 9

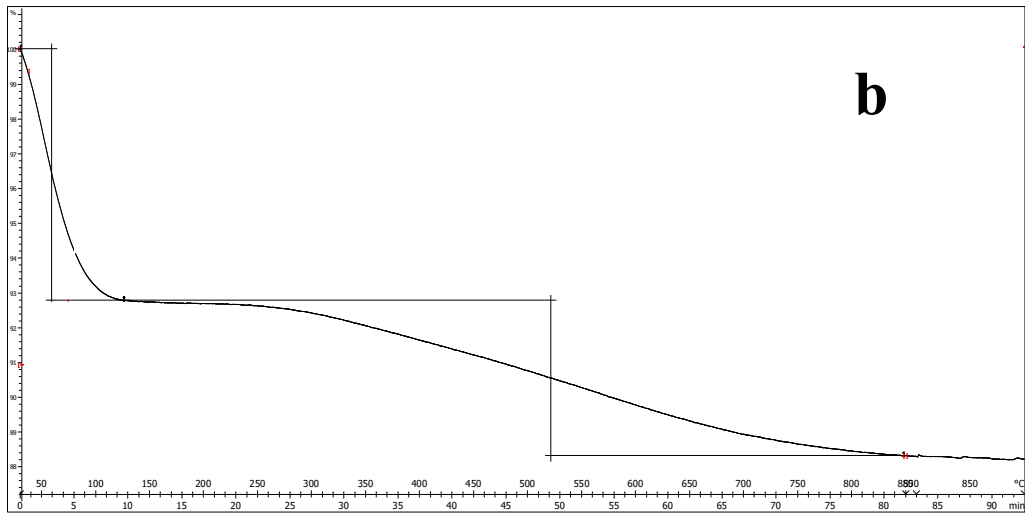
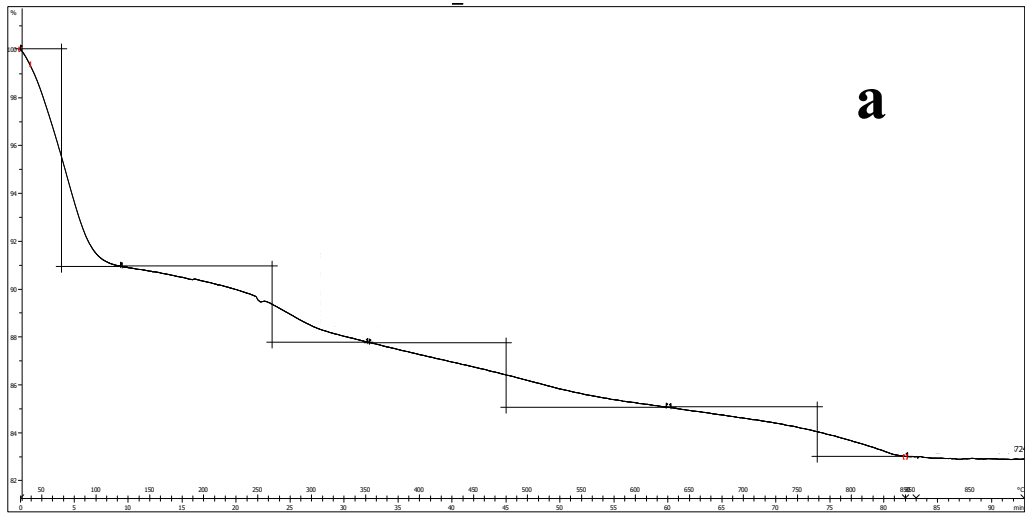


FIGURE 10

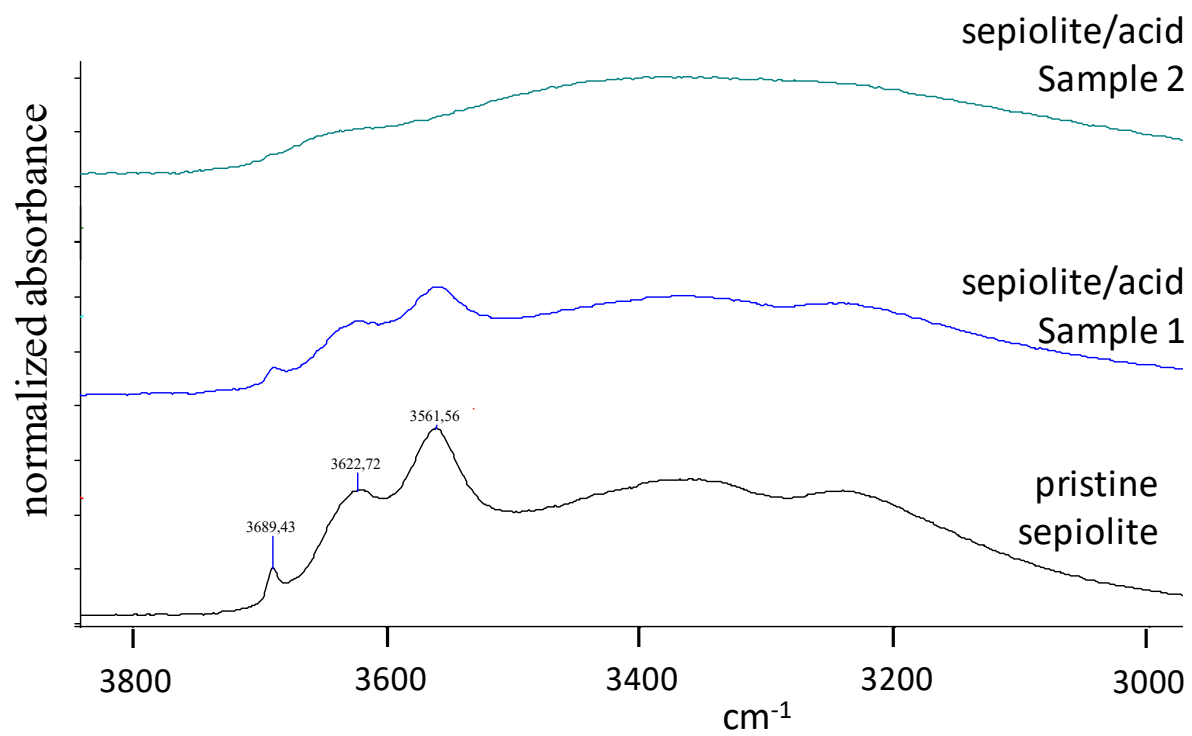


FIGURE 11

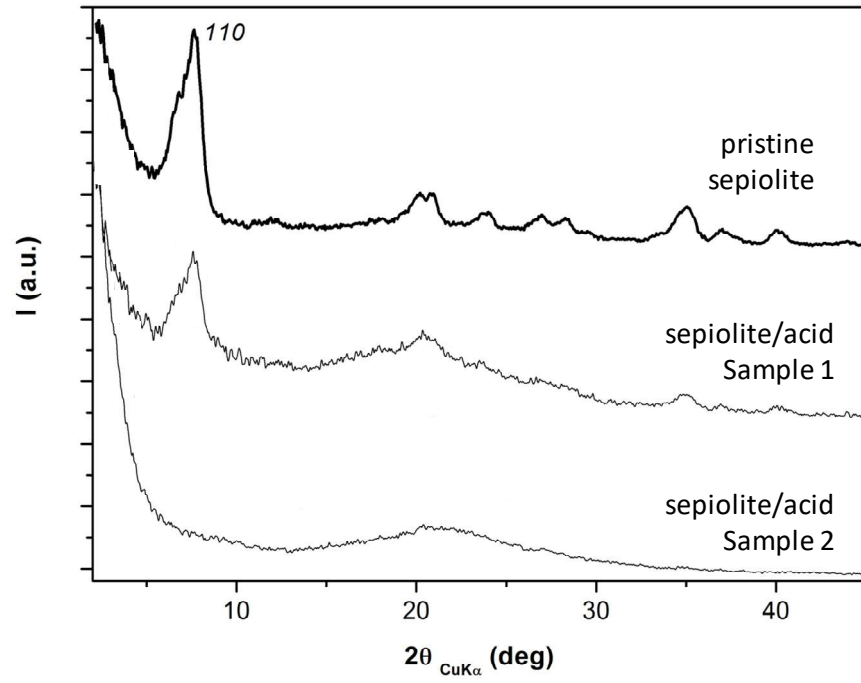


FIGURE 12

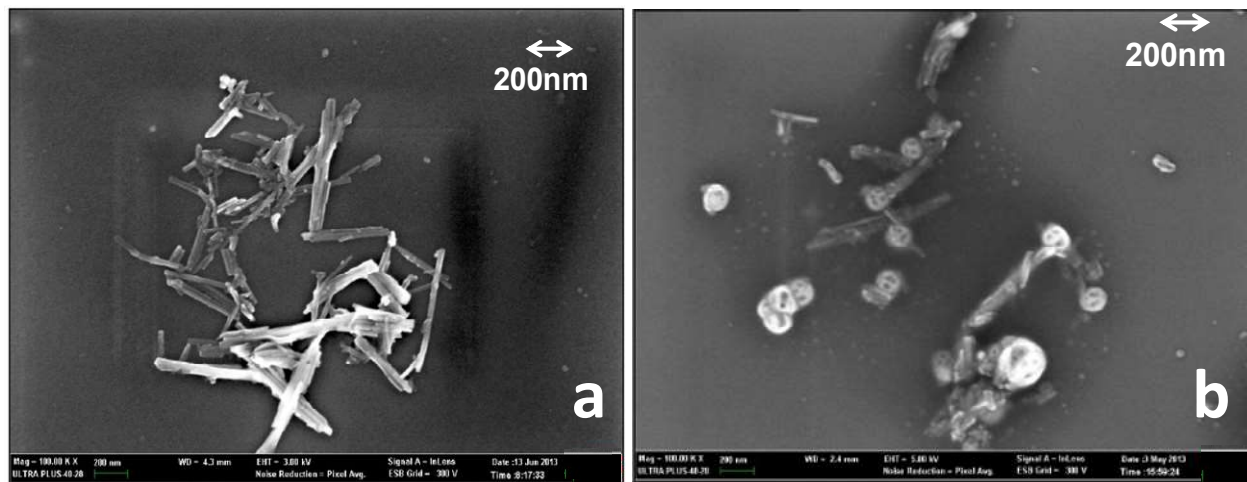
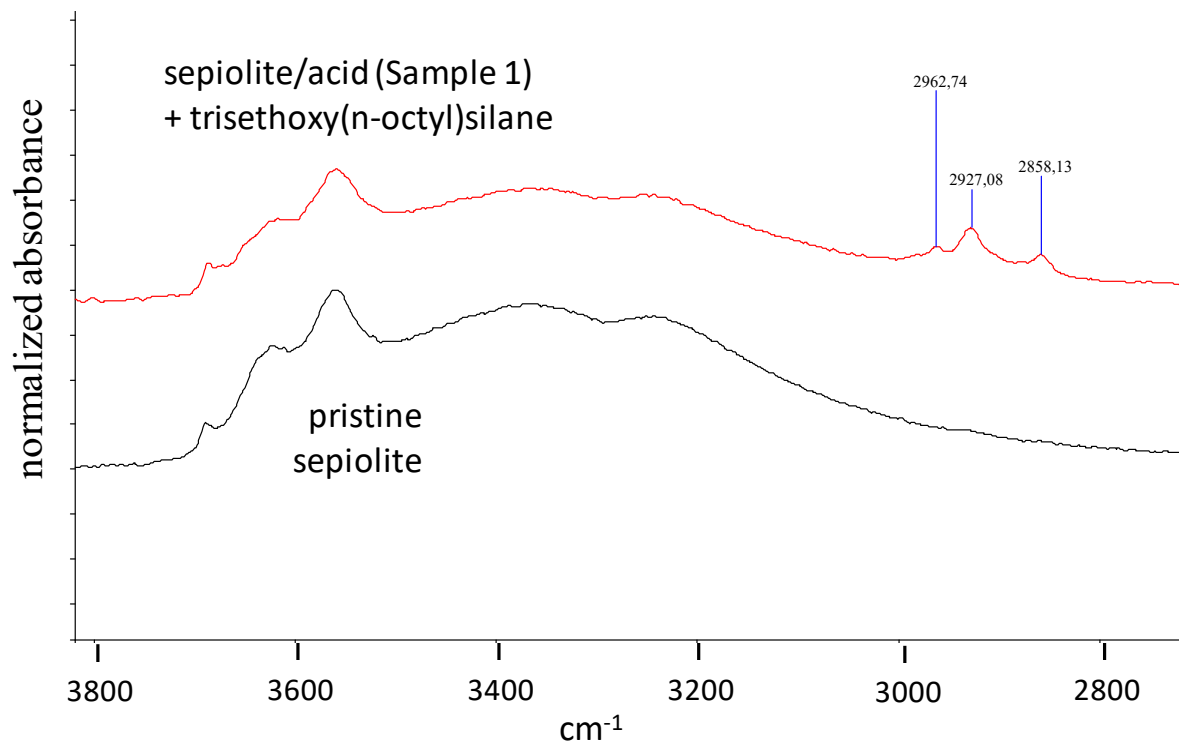


FIGURE 13



LIST OF FIGURE CAPTIONS

Figure 1. 2-(2,5-dimethyl-1*H*-pyrrol-1-yl)-1,3-propanediol (serinolpyrrole, SP).

Figure 2. The structure of sepiolite

Figure 3. Experimental procedure for the treatment of Sepiolite with tetraethyl orthosilicate

Figure 4. TGA curves of silica, pristine sepiolite and sepiolite/TEOS

Figure 5. ATR-IR spectra of pristine sepiolite and sepiolite/TEOS in the 2800-3800 cm^{-1} region

Figure 6. X-ray patterns of pristine sepiolite and sepiolite/TEOS

Figure 7. FESEM of pristine sepiolite (a) and of sepiolite/TEOS (b)

Figure 8. Experimental procedure for the treatment of Sepiolite with HCl aq solution

Figure 9. TGA curves of sepiolite treated with acid: (a) Sample 1 (10 min at 60°C), (b) Sample 2 (70 min at 60°C).

Figure 10. ATR-IR spectra in the 3000-3800 cm^{-1} region of pristine sepiolite and sepiolite treated with acid: Sample 1 (10 min at 60°C), Sample 2 (70 min at 60°C).

Figure 11. X-ray patterns of pristine sepiolite and sepiolite treated with acid: Sample 1 (10 min at 60°C), Sample 2 (70 min at 60°C)

Figure 12. FESEM of sepiolite treated with acid: (a) Sample 1 (10 min at 60°C), (b) Sample 2 (70 min at 60°C)

Figure 13. ATR-IR spectra of pristine sepiolite and sepiolite/acid (Sample 1) silanized with

TABLE I

FILLERS: MAIN FEATURES AS A FUNCTION OF THE PARTICLE DIAMETER

Particle diameter (nm)	10	1000
Particles / cc (number)	$1.9 \cdot 10^7$	$1.9 \cdot 10^{11}$
Internal surface area / cc (m ²)	60	0.6
Average interparticle distance (nm)	8.5	850

TABLE IIMASS LOSSES FOR SILICA, PRISTINE SEPIOLITE, SEPIOLITE TREATED WITH TEOS^a

	Mass losses in different T (°C) ranges				Residue
	T < 150	150 < T < 400	400 < T < 700	700 < T < 850	
Silica	5.0	=	=	=	95.0
Pristine Sepiolite	9.0	3.4	3.4	2.6	82.0
Sepiolite / TEOS	7.0	2.8	4.2	2.6	83.8

^a from TGA analysis

TABLE III

FORMULATIONS OF NR BASED COMPOSITES WITH SILICA AND SEPIOLITE
TREATED WITH TEOS^a

Ingredient	Filler(s) in the composite		
	Silica	Silica + Sepiolite	Silica + sepiolite/TEOS
NR	100	100	100
Silica	45	35	35
Sepiolite	0	10	0
Sepiolite/TEOS	0	0	10
Silane TESPT	3.6	3.6	3.6
Stearic acid	2	2	2
ZnO	3.6	3.6	3.6
6PPD	2	2	2
S	2.8	2.8	2.8
TBBS	1.8	1.8	1.8

^a All the quantities of the ingredients are expressed in phr = parts per hundred rubber.

TABLE IV

$G'_{\gamma_{min}}$, $\Delta G'/G'$, Tan delta max FOR NR BASED COMPOSITES WITH SILICA AND SEPIOLITE TREATED WITH TEOS

Property	Filler(s) in the composite		
	Silica	Silica + Sepiolite	Silica + sepiolite/TEOS
$G' (0.4\%)$	1.51	1.48	1.28
$\Delta G' (0.4\%-35\%)/G' (0.4\%)$	0.30	0.31	0.26
Tan Delta max	0.071	0.074	0.067

TABLE V
TENSILE PROPERTIES FOR NR BASED COMPOSITES WITH SILICA AND SEPIOLITE
TREATED WITH TEOS

Property	Filler(s) in the composite		
	Silica	Silica + Sepiolite	Silica + sepiolite/TEOS
σ_{50} (MPa)	1.45	2.47	1.72
σ_{100} (MPa)	2.91	5.63	4.12
σ_{300} (MPa)	16.76	18.5	18.08
σ_B (MPa)	21.57	23.39	22.04
ϵ_B (%)	361.05	371.34	365.07

TABLE VI

SEPIOLITE. EXTRACTED Mg UPON TREATMENT WITH HCl

Sample	Treatment time		Extracted Mg	
	(min)	mmol/(g of sepiolite)		%
1	10	2.1		33.8
2	70	5.1		82.6

TABLE VIIMASS LOSSES FOR PRISTINE SEPIOLITE AND SEPIOLITE TREATED WITH HCl^a

	Mass losses in different T (°C) ranges				Residue
	T < 150	150 < T < 400	400 < T < 700	700 < T < 850	T > 850°C
Pristine Sepiolite	9.0	3.3	3.3	2.3	82.1
Sepiolite / HCl Sample 1	9.0	3.2	2.7	2.0	83.1
Sepiolite / HCl Sample 2	7.2	=	=	4.5	88.3

^a Sepiolite treated with HCl at 60°C: Sample 1 for 10 min, Sample 2 for 70 min

TABLE VIII

TRIETHOXY(OCTYL)SILANE IN ADDUCTS WITH SILICATE

Silicate	Silane in the final adduct (mass%)^a
Silica	4.1
Pristine sepiolite	3.5
Acid treated sepiolite. Sample 1	4.0

^ainitial amount of silane in sepiolite: 10% by mass

TABLE IX

FORMULATIONS OF NR BASED COMPOSITES WITH SILICA AND SEPIOLITE
TREATED WITH ACID^a

Ingredient	Filler in the composite		
	Silica	Silica + Sepiolite	Silica + Sepiolite (Sample 1)
NR	100	100	100
Silica	45	35	35
Sepiolite	0	10	0
Sepiolite/TEOS	0	0	10
Silane TESPT	3.6	3.6	3.6
Stearic acid	2	2	2
ZnO	3.6	3.6	3.6
6PPD	2	2	2
S	2.8	2.8	2.8
TBBS	1.8	1.8	1.8

^a All the quantities of the ingredients are expressed in phr = parts per hundred rubber.

TABLE X

$G'_{\gamma_{min}}$, $\Delta G'/G'$, Tan delta max FOR NR BASED COMPOSITES WITH SILICA AND SEPIOLITE TREATED WITH ACID

Property	Filler in the composite		
	Silica	Silica + Sepiolite	Silica + Sepiolite (Sample 1)
$G' (0.4\%)$	1.51	1.48	1.31
$\Delta G' (0.4\%-35\%)/G' (0.4\%)$	0.30	0.31	0.27
Tan Delta max	0.071	0.074	0.071

TABLE XI

TENSILE PROPERTIES FOR NR BASED COMPOSITES WITH SILICA AND SEPIOLITE

Property	Filler in the composite		
	Silica	Silica + Sepiolite	Silica + Sepiolite (Sample 1)
σ_{10} (MPa)	0.48	0.62	0.50
σ_{50} (MPa)	1.45	2.47	1.67
σ_{100} (MPa)	2.91	5.63	3.79
σ_{300} (MPa)	16.76	18.50	16.68
σ_B (MPa)	21.57	23.39	21.94
ε_B (%)	361.05	371.34	376.85